Model-Free Measurement of the Excited-State Fraction in a ^{85}Rb Magneto-Optical Trap

G. Veshapidze,[1] J.-Y. Bang,[2] C. W. Fehrenbach,[2] H. Nguyen,[3] and B. D. DePaola[2]

[1]*School of Natural Sciences and Engineering, Ilia State University, Tbilisi 0162, Georgia**
[2]*Department of Physics, Kansas State University, Manhattan, Kansas 66506-2601*
[3]*Department of Physics, University of Mary Washington, Fredricksburg, VA 22401*

(Dated: May 1, 2015)

In many experiments involving magneto-optical traps (MOTs), it is imperative to know the fraction of atoms left in an excited state by the cooling and trapping lasers. In most cases, researchers have used formulas that were derived for simple 2-level systems interacting with a single beam of light having a well-defined polarization, and in the absence of magnetic or electric fields. However a MOT environment is much more complex than this. Here we directly measure the excited fraction in a MOT of ^{85}Rb atoms in a model-independent manner for a wide range of trapping conditions. We then fit our measured fractions to an ansatz based on a simple model. Knowing only the trapping laser's total intensity and detuning from resonance, one can then use this ansatz to accurately predict the excited fraction. The work is a companion piece to similar measurements on a MOT of ^{87}Rb.

PACS numbers: 32.80.Pj, 32.80.-t, 32.60.+i, 32.10.Gh

I. INTRODUCTION

Magneto optical traps (MOTs) have become a workhorse for measuring many optical properties of atoms and molecules. Very often in these measurements it is necessary to know the fraction of atoms that are in an excited state from their interaction with the cooling and trapping lasers. In most cases, to estimate the fraction of atoms in an excited state, the complex environment of a MOT has been approximated by a low density atomic target in a field-free space, and with a single beam of light having a well-defined polarization. In this case, the solution of the optical Bloch equations yields a steady state excited fraction given by[1, 2]

$$f = \frac{(\Omega/\Gamma)^2}{1 + 2\,(\Omega/\Gamma)^2 + (2\delta/\Gamma)^2}, \tag{1}$$

where Ω is the Rabi frequency at resonance[3], δ is the laser detuning from resonance, and Γ is the transition line width.[4] With (see footnote [5])

$$\left(\frac{\Omega}{\Gamma}\right)^2 = \frac{I}{2I_s}, \tag{2}$$

Eq. (1) becomes

$$f = \frac{I/\,(2I_s)}{1 + I/I_s + (2\delta/\Gamma)^2}. \tag{3}$$

Here I is the laser intensity, and I_s is the saturation intensity. Equation (3) can also be written in terms of a single saturation parameter, s:

$$f = \frac{s}{1+2s} \tag{4a}$$

$$s \equiv \frac{I/(2I_s)}{1 + (2\delta/\Gamma)^2}. \tag{4b}$$

Depending on the number of laser beams used, their polarization, the number of hyperfine sub-levels one considers in the model, and the degree of optical pumping, I_s can take on values ranging from 1.7 to 3.9 mW/cm^2. For a 3-D optical molasses, with no magnetic fields, the value $I_s = 3.895$ mW/cm^2 is often used, though according to Steck[2], "this is almost certainly an overestimate of the effective saturation intensity since sub-Doppler cooling mechanisms will lead to optical pumping and localization in the light maxima". In the absence of more specific theoretical or experimental guidance, this value for I_s is also often used with Eq. (3) in order to estimate the excited fraction in a MOT. A summary of theoretical values of I_s for different excitation conditions is given on the left side of Table I.

More sophisticated models for computing the excited fraction in a MOT do exist. Recognizing that the use of Eq. (1) was overly simplistic, Townsend *et al.* [9] proposed that the excited fraction could be estimated by

$$f = \frac{C_1^2 I/I_s}{1 + 2C_2^2 I/I_s + (2\delta/\Gamma)^2}, \tag{5}$$

where C_1^2 and C_2^2 are Clebsch-Gordon (CG) coefficients, averaged over all possible polarizations and m_F.

Javanainen [10] modeled population dynamics in a MOT and fit his calculated populations to the ansatz:

*Corresponding author email: giorgi.veshapidze@iliauni.edu.ge

TABLE I: Summary of theoretical and experimental values for the saturation intensity, I_s, and the valid range of scaled intensity s'. Column a is for a single σ-polarized laser beam on the cycling transition; b is for a single π-polarized laser beam on the cycling transition; c is for a 1-D optical molasses; d is for a single "isotropically polarized" beam; e is for a far-detuned π-polarized beam. Theory values are from Steck[2, 6].

	Theoretical values of I_s (mW/cm^2)				Experiment (mW/cm^2)		
	a	b, c	d	e	Other[7]	This Work	Valid range of s'
^{85}Rb	1.66932(35)	3.12950(57)	3.89509(81)	2.50399(52)	5.25	3.7(4)	0.5 - 4.0
^{87}Rb[8]	1.66933(35)	3.05381(53)	3.57713(74)	2.50399(52)	4.55	4.6(9)	< 5.75

$$f = \frac{y}{1+2y}, \tag{6a}$$

$$y \equiv \left[\left(\alpha^{-1} - \beta^{-1}\right)\frac{s_r}{s+s_r} + \beta^{-1}\right] s, \tag{6b}$$

where α, β, and s_r are fitted parameters, and s is the saturation parameter of Eq. (4b). Here $\alpha^{-1/2}$ and $\beta^{-1/2}$ are effective CG coefficients at low and high values of s, respectively. The parameter s_r is used to define what one means by "high" and "low." Note that for $s \ll s_r$, $y \to s/\alpha$, and for $s \gg s_r$, $y \to s/\beta$. Thus, for extreme values of s, Eqs. (6) become equivalent to Eq. (1), but with an effective saturation intensity given by αI_s or βI_s.

In earlier work [11] we directly measured the excited fraction in cooled and trapped ^{87}Rb. We found that Eqs. (4) correctly model the excited fraction in a MOT over a wide range of trapping and cooling conditions, *but substituting a fitted value of I_s rather than one of the values given in Table I.* Because Eq. (1) is a special case of Eqs. (5) and (6), those models also worked with a fitted value of I_s, but not better than the simpler case of Eqs. (4). The results of the ^{87}Rb measurements are shown in Table (I).[8]

In this work, we build on the ^{87}Rb results by directly measuring the excited fraction in a ^{85}Rb MOT over a range of cooling and trapping conditions and using those data to obtain a fitted value of I_s. As Eqs. (5) or (6) imply, we expect this fitted value to be different for ^{85}Rb than for ^{87}Rb because different hyperfine levels are involved. Finally, we conclude this work by revisiting the ^{87}Rb case in order to present all Rb results in a single table.

II. EXPERIMENTAL PROCEDURE

We follow the same experimental procedure as used in the ^{87}Rb measurements.[11] This is a charge transfer methodology known as MOTRIMS (magneto-optical trap recoil ion spectroscopy).[12] In MOTRIMS, atoms are cooled and trapped and are then used as a target for a beam of photons or ions; here we use a beam of 7 keV Na^+. When charge transfer occurs, the neutral Na atom and the Rb^+ ion are detected by two separate 2-dimensional position-sensitive detectors. From conservation of energy and momentum, the component of the recoil ion momentum that lies along the collision axis, $p_\parallel$,

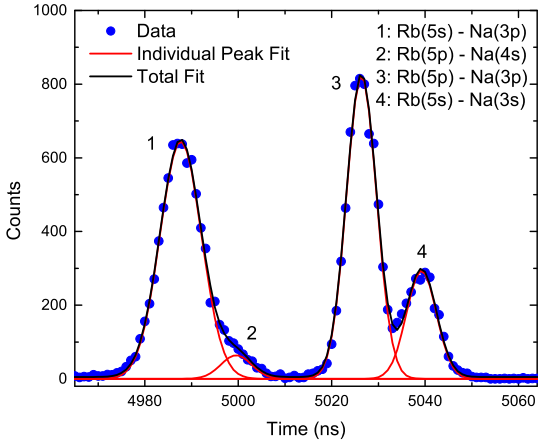

FIG. 1: (Color online) Typical time-of-flight spectrum from which the excited fraction is determined. The peak labeled "1" is dominated by the Rb(5s) → Na(3p) channel, but actually has contributions from other smaller channels. The peak labeled 3 is due to charge transfer from Rb(5p) → Na(3p), while the peak labeled 4 is due to charge transfer from Rb(5s) → Na(3s). These last two peaks were used to deduce the excited fraction. (See text for details.) In the fitting procedure, the widths of peaks 3 and 4 were constrained to be equal and represent the instrumental resolution.

is directly related to the so-called Q-value of the collision by

$$Q = -v_p p_\parallel - m_e v_p^2/2, \tag{7}$$

where v_p is the projectile ion velocity, m_e is the electron mass, and the Q-value is defined as the difference between the binding energy of the transferred electron before and after the collision and, for simple systems like the alkalis, uniquely identifies the charge transfer channel. For the geometry of our apparatus, $p_\parallel$ is determined by the flight time of the recoiling Rb^+, while v_p is insignificantly changed in the collision; therefore, Q can be determined from just the time of flight spectrum.[13] Because the ion-atom interactions are so weak, perturbation of the excited fraction by the Na^+ beam is negligible. A typical time-of-flight spectrum is shown in Fig. (1). The rightmost peak in Fig. (1) is due to electron transfer from Rb(5s) to Na(3s); in what follows, we refer to this by the

label "ss". The peak immediately to the left of the ss peak is due to charge transfer from Rb(5p) to Na(3p); we refer to this by the label "pp". The relative areas of the ss and pp peaks are proportional to the populations in Rb(5s) and Rb(5p) states, respectively, before the charge transfer collision. That is,

$$A_{if} \propto N_i \sigma_{if}, \tag{8}$$

where A_{if} is the area of the peak corresponding to charge exchange from initial state i to final state f, N_i is the number of atoms in the initial state, and σ_{if} is the cross section for that charge transfer channel. The measured excited fraction fraction, then, is given by

$$f_m = \frac{A_{pp}/\sigma_{pp}}{A_{pp}/\sigma_{pp} + A_{ss}/\sigma_{ss}} = \frac{A_{pp}}{A_{pp} + RA_{ss}}, \tag{9a}$$

$$R \equiv \frac{\sigma_{pp}}{\sigma_{ss}}. \tag{9b}$$

The ratio of cross sections for this system and at this collision energy was previously measured [14] and all other proportionality constants, such as detection efficiency, cancel out. Thus, simply measuring the ratio of the ss and pp peak areas gives a model-free value for the excited fraction in the MOT for any given laser intensity, detuning, alignment condition, etc.

Besides the fitted parameter I_s, Eq. (4b) contains two independent variables, the trapping laser's detuning from resonance δ and the trapping laser's intensity I. The trapping laser was locked to the 2-4 cross-over peak in a saturation absorption spectrum, placing it 92 MHz to the red of the $F = 3$ to $F' = 4$ trapping transition.[2] After passing through a single-mode optical fiber, light from the trapping laser was single-passed through an acousto-optic modulator (AOM), which allowed control of the parameter δ. After passing through the AOM, the light was expanded and collimated before being split into three parts using polarization optics. The three beams were sent into the trapping chamber on orthogonal axes and retro-reflected, giving a total of six trapping beams. Since the AOM was placed in the focus of a 1:1 telescope, the change in the deflection angle, induced by the AOM was translated into a lateral shift of the beam. This shift, for the range of detunings investigated, was negligibly small compared with the laser beam diameter at the MOT location.

The repump laser was locked to the $F = 2$ to $F' = 3$ transition in a saturation-absorption spectrum and combined with the trapping beam just upstream of the collimation-beam expansion optics. Beam spot sizes were measured using a variation on the scanning slit method.[15] Since we were unable to measure the trapping beam size at the location of the MOT (inside the vacuum chamber), we estimated the distance of the MOT from some reference point along the trapping beam and measured the beam size at the equivalent distance from the same reference point by rerouting the beam outside the chamber. We repeated this procedure for all direct and retroreflected beams. The power in the repump laser as well as in the three trapping beams were measured upstream from the trapping chamber. Reflectivity of the chamber windows as well as the retro-reflection optics were measured and accounted for in deducing the trapping and repump laser intensities at the MOT location. As in the ^{87}Rb measurements[11] peak intensities were used. This is justified because, as is usually the case for MOTs, the cloud of cooled trapped atoms is small compared to the diameter of the trapping laser beams. Thus the atoms are exposed to laser light having the sum peak intensities of the combined trapping laser beams.

In a typical run the AOM was stepped through 16 frequencies and the trapping laser intensity was measured for each AOM frequency. Some slight optical power variation with frequency was observed and used in the fit, but the laser power was otherwise held fixed on a given run. A variable neutral density filter was put in the trapping laser beam to vary the trapping laser power for different scans of AOM frequency.

Besides varying trapping laser intensity and detuning, the ratios of the power in the three trapping legs was also varied. Usually, the ratio was 2:2:1, where the weakest leg was the one that entered the chamber along the axis of the trap's anti-Helmholtz coils. However excited fractions for ratios of 1:1:1 were also measured.

Note that the ion beam diameter is roughly the same size as the MOT diameter and therefore samples the entire MOT. Moving the MOT with respect to the ion beam axis resulted in a lower charge transfer rate, but not in a change in measured excited fraction. We therefore conclude that spatial variations in excited states, if they exist at all, are on a length scale that is much smaller than the MOT.

III. RESULTS

Figure (2) shows measured excited fractions plotted versus a scaled intensity given by

$$s' = \frac{I/2}{1 + (2\delta/\Gamma)^2}. \tag{10}$$

Note that the scaled intensity s' differs from the usual saturation parameter of Eq. (4b) only in that it has not been divided by I_s. Thus, unlike s which is dimensionless, s' has units of intensity. For I we use the sum of the peak intensities for all trapping (but not repump) laser beams. The vertical error bars in Fig. (2) are given by

$$\frac{\Delta f_m}{f_m} = (1 - f_m)\sqrt{\left(\frac{\Delta A_{pp}}{A_{pp}}\right)^2 + \left(\frac{\Delta A_{ss}}{A_{ss}}\right)^2 + \left(\frac{\Delta R}{R}\right)^2}. \tag{11}$$

Non-systematic uncertainty in s' is smaller than the size of the data points and is therefore not shown.

The broken curves in Fig. (2) refer to theoretical values of I_s from the left side of Table I. The solid line represents

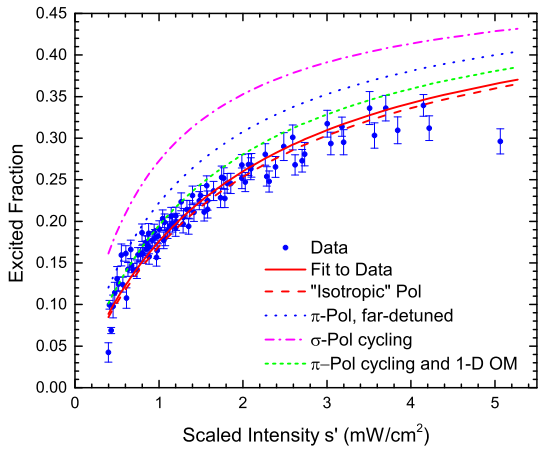

FIG. 2: (Color online) Measured excited fractions. The points are measured data. The broken curves are from Eqs. (4) for the different values of I_s given on the left side of Table I. The solid line is the best fit of Eq. (12) to the data; the resulting value for I_s is given on the right side of Table I.

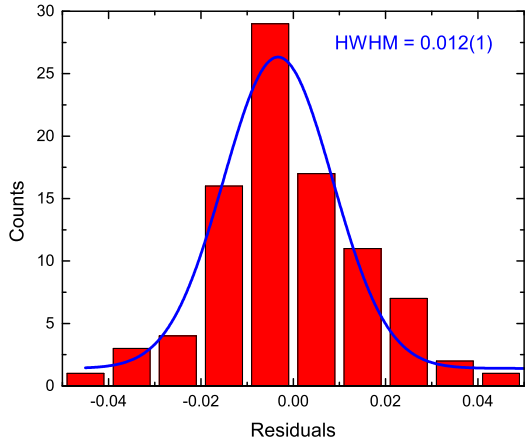

FIG. 3: (Color online) Histogram of the residuals from Fig. (2), with respect to the recommended fit (the solid line).

the best fit to the data. To be explicit, the fitting function is

$$f_{\rm fit} = \frac{s'/I_s}{1 + 2s'/I_s}, \tag{12}$$

where now I_s is the fitting parameter. The fitted value of I_s is 3.67(6), where the error comes from the goodness of fit and reflects both the error in the measured excited fraction and the statistical scatter of the data.

Figure (3) is a histogram of residuals from the solid line fit in Fig. (2). A Gaussian fit to the histogram gives a half-width-half-max (HWHM) of 0.012. For a typical excited fraction of 0.20, this implies a fit error of 0.012/0.20.

The fit error of I_s does not include systematic error in either laser intensity or detuning. The systematic error can be included using

$$\left(\frac{\Delta I_s}{I_s}\right)_{\rm tot} = \sqrt{\left(\frac{\Delta I_s}{I_s}\right)^2_{\rm fit} + \left(\frac{\Delta I}{I}\right)^2 + \left(\frac{2(2\delta/\Gamma)^2}{1+(2\delta/\Gamma)^2}\right)^2 \left(\frac{\Delta\delta}{\delta}\right)^2}, \tag{13}$$

where the subscripts "fit" and "tot" indicate fitted and total errors, respectively. Usually, in the case of a MOT, $2\delta \gg \Gamma$, and Eq. (13) becomes

$$\left(\frac{\Delta I_s}{I_s}\right)_{\rm tot} \approx \sqrt{\left(\frac{\Delta I_s}{I_s}\right)^2_{\rm fit} + \left(\frac{\Delta I}{I}\right)^2 + 4\left(\frac{\Delta\delta}{\delta}\right)^2}. \tag{14}$$

Since the peak-locking method was used for the laser frequency locking, the main contributor to the $\Delta\delta$ would be the unknown but small stray magnetic field at the MOT position, inducing corresponding Zeeman shifts, and uncertainty in the measurement of the AOM frequency, that was used to apply different frequency shifts to the trapping laser, during measurement.

The largest contributor to the total error in I_s is the uncertainty in the trapping laser intensity, due to the relatively imprecise estimation of the MOT position (see Experimental Procedures). Including the systematic error in the measurements of trapping laser intensity and detuning in the Eq. (14) yields $I_s(^85Rb) = 3.7(4)$, as listed in Table I.

In earlier work[11] with ^{87}Rb, the data tended to depart from this simple fit at the highest saturation parameters. In the present data, there is still a hint of this trend. The data also seem to drop below the fitted curve at the lowest values of saturation parameter. It was difficult to probe higher values of s' because of power limitations of the trapping laser. Furthermore, increasing s' by decreasing detuning from resonance weakened the MOT so badly that charge transfer rate was prohibitively low. Similarly, exploring smaller values of s' was problematic because increasing δ or decreasing I resulted in a weak MOT and consequent poor counting statistics. Nevertheless, we can say that for $0.5 \leq s' \leq 4$, and for a fitted value of $I_s = 3.67$ mW/cm^2, Eqs. (4) fit the data quite well. The valid range of s' for use of the fitted I_s is shown in the final column of Table I.

When using the recommended value of I_s from this work for ^{85}Rb, or the value of I_s for ^{87}Rb from the earlier work[11], the uncertainty in the estimated value of excited fraction, f_e, is given by

$$\frac{\Delta f_e}{f_e} = (1-2f_e)\sqrt{\left(\frac{\Delta I}{I}\right)^2 + \left(\frac{\Delta I_s}{I_s}\right)^2_{\rm tot} + \left(\frac{2(2\delta/\Gamma)^2}{1+(2\delta/\Gamma)^2}\right)^2\left(\frac{\Delta\delta}{\delta}\right)^2}. \quad (15)$$

Or, for large detuning, $2\delta \gg \Gamma$,

$$\frac{\Delta f_e}{f_e} \approx (1-2f_e)\sqrt{\left(\frac{\Delta I}{I}\right)^2 + \left(\frac{\Delta I_s}{I_s}\right)^2_{\rm tot} + 4\left(\frac{\Delta\delta}{\delta}\right)^2}. \quad (16)$$

The ^{85}Rb and ^{87}Rb experiments differed in one significant aspect: Sensitivity to the repump laser intensity. As is well-known, the separation between the upper two hyperfine lines in ^{85}Rb($5p_{3/2}$) is much less than in ^{87}Rb($5p_{3/2}$), (121 MHz *versus* 267 MHz) leading to more pronounced optical pumping to the ground hyperfine state by the trapping laser for ^{85}Rb. Thus, the intensity requirements on the repump laser are more severe for ^{85}Rb than for ^{87}Rb. Not surprisingly, optical pumping also decreases the excited fraction since an atom in an inadequately repumped ground hyperfine state has less chance to be excited. However, what is surprising is that the excited fraction seems even more sensitive to repump intensity than is the number of atoms contained in the MOT. Figure (4) shows a plot of both excited fraction (circles) and MOT population (triangles) *versus* repump laser intensity. The "population" is actually just the sum of A_{ss}/σ_{ss} and A_{pp}/σ_{pp} which should be proportional to the total number of atoms in the MOT.[16] Within the scatter in the population data, it remains unchanged over the same range of repump laser intensities that gave rise to a 30% increase in excited fraction. (The data of Fig. (2) were all taken at repump intensities of 3.5 mW/cm^2, which is well within the plateau region beyond the critical knee at 2.5 mW/cm^2 in Fig. (4).) Those who wish to use the empirical results here to estimate the excited fraction in their ^{85}Rb MOTs would be well advised to apply at least this repump laser intensity.

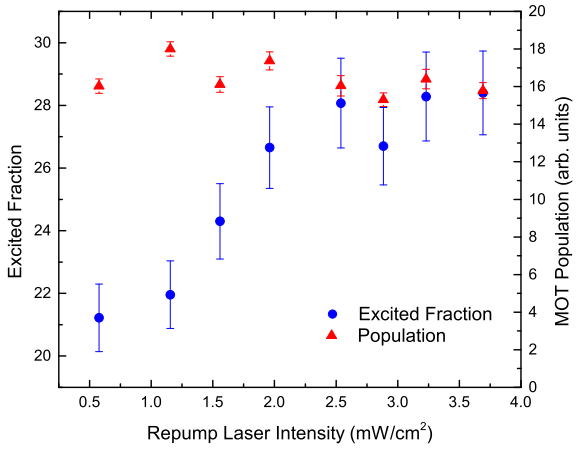

FIG. 4: (Color online) Excited fraction (circles) and number of atoms in the MOT (triangles) as a function of repump laser intensity. The MOT population is in arbitrary units.

IV. SUMMARY

Model-free measurements were made of the excited fraction for ^{85}Rb in a MOT. As in the case for ^{87}Rb, the solution to the optical Bloch equations for a simple 2-level system provided a good fit to the data, but with

an empirically determined effective saturation intensity. The results of this work and earlier work on ^{87}Rb are summarized in the right side of Table I.

As long as the trapping conditions are within the valid range of s', where s' is the scaled intensity defined in Eq. (10), use of the recommended value of I_s for this work should lead to an error in an estimate of the excite fraction as low as $\Delta f_e \geq (0.1) f_e(1-f_e)$, where the pre-factor is the error in I_s, and this best-case scenario is for zero uncertainty in the user's laser intensity and detuning. For an excited fraction of 0.2, this leads to $\Delta f_e/f_e \approx 0.06$, that is, $f_e = 0.20(6)$. The oft-used value for I_s listed in column a of Table I can lead to a systematic error of 0.10 in the fraction of atoms in the excited states (i.e. more than 50% higher than our directly measured fraction). Though use of the "best" theoretical value of I_s, given in column d, e of Table I, predicts excited fractions very close to those predicted by this work, differing by only one or two percent from the I_s recommended in this work, it does not predict the limited validity in the range of scaled intensity s'.

Finally we would like to note, that the measured values of I_s for ^{85}Rb and ^{87}Rb, agree with each other, within error, as expected theoretically.

Acknowledgments

GV wishes to acknowledge the Shota Rustaveli National Science Foundation, under contract No. 04/04.

[1] W. Demtröder, *Laser Spectroscopy: Basic Concepts and Instrumentation* (Springer, Berlin, 2002).

[2] D. A. Steck, *Rubidium 85 d line data, revision 2.1.5* (2012), URL `http://steck.us/alkalidata`.

[3] B. W. Shore, *Theory of Coherent Atomic Excitation* (John Wiley and Sons, 1990).

[4] Here δ and Γ are both expressed either as angular or linear frequencies.

[5] The literature shows an ambiguity by a factor of 2 in the definition of I_s. Reference [1] uses one definitation, while ref. [2] uses the other. In the present work we opt for what seems to be the most common preference in today's literature, namely that of Steck[2].

[6] D. A. Steck, *Rubidium 87 d line data, revision 2.1.4* (2010), URL `http://steck.us/alkalidata`.

[7] T. P. Dinneen, C. D. Wallace, K.-Y. N. Tan, and P. L. Gould, Opt. Lett. **17**, 1706 (1992), URL `http://ol.osa.org/abstract.cfm?URI=ol-17-23-1706`.

[8] The data for ^{87}Rb have been adjusted from the published[11] numbers in order to reflect the definition of I_s used in the present work. The same has been done for the column labeled "Other".

[9] C. G. Townsend, N. H. Edwards, C. J. Cooper, K. P. Zetie, C. J. Foot, A. M. Steane, P. Szriftgiser, H. Perrin, and J. Dalibard, Phys. Rev. A **52**, 1423 (1995), URL `http://link.aps.org/doi/10.1103/PhysRevA.52.1423`.

[10] J. Javanainen, J. Opt. Soc. Am. B **10**, 572 (1993), URL `http://josab.osa.org/abstract.cfm?URI=josab-10-4-572`.

[11] M. H. Shah, H. A. Camp, M. L. Trachy, G. Veshapidze, M. A. Gearba, and B. D. DePaola, Phys. Rev. A **75**, 053418 (2007), URL `http://link.aps.org/doi/10.1103/PhysRevA.75.053418`.

[12] B. DePaola, R. Morgenstern, and N. Andersen (Academic Press, 2008), vol. 55 of *Advances In Atomic, Molecular, and Optical Physics*, pp. 139 – 189, URL `http://www.sciencedirect.com/science/article/pii/S1049250X07550032`.

[13] Detection of the neutralized Na projectile starts a time-to-digital converter (TDC) and detection of the recoiling Rb^+ ion provides the stop signal. The TDC spectrum therefore has a temporal offset consisting of the extra time it takes the projectile to leave the collision region and strike its detector. This is of no consequence to the excited fraction measurement.

[14] T. G. Lee, H. Nguyen, X. Flechard, B. D. DePaola, and C. D. Lin, Phys. Rev. A **66**, 042701 (2002), URL `http://link.aps.org/doi/10.1103/PhysRevA.66.042701`.

[15] G. Veshapidze, M. L. Trachy, M. H. Shah, and B. D. DePaola, Appl. Opt. **45**, 8197 (2006), URL `http://ao.osa.org/abstract.cfm?URI=ao-45-32-8197`.

[16] Though this method of measuring variations in the total number of atoms in the MOT is reasonable for a few short runs, it may not be reliable in comparing day to day variations in population since the ion beam could vary in which portions of the MOT it probes. However, the measured excited *fraction* is independent of these variations.